

Relativistic corrections to energy spectrum of hydrogen due to the full one-photon-exchange interaction

Zi-Wen Zhang and Hai-Qing Zhou*

School of Physics, Southeast University, NanJing 211189, China

(Dated: March 8, 2024)

In this work, we estimate the relativistic corrections to the energy spectrum of hydrogen resulting from the full one-photon-exchange interaction using a highly precise numerical method. In the frame of the effective Schrodinger-like equation, which is derived exactly from the Bethe-Salpeter equation in quantum electrodynamics, we express the effective potential corresponding to the full one-photon-exchange interaction in terms of eight scalar functions. Unlike the usual calculations performed in the references, where the effective potential is expanded in terms of momenta order by order, we retain the exact momentum dependence in the effective potential to estimate its corrections to the energy spectrum of hydrogen using a highly precise numerical method. We also use the same numerical method to double-check the results in the non-relativistic case to ensure accuracy. We discuss the comparison of the numerical results with those obtained using the usual bound-state perturbative theory. Our calculations suggest that it is possible to accurately account for all the relativistic contributions using this method. It would be interesting to extend these calculations to positronium, muonic hydrogen, and cases involving nuclear structure and radiative corrections.

I. INTRODUCTION

The study of the energy spectrum of hydrogen-like atoms has been pivotal in the development of quantum mechanics and has remained important for over a century. However, dealing with bound states in a pure quantum field theory, especially when the non-relativistic expansion is not valid, can still be challenging. In the past fifteen years, there have been significant improvements in the precise experimental measurements of

* E-mail: zhouhq@seu.edu.cn

the Lamb shifts of hydrogen and muonic hydrogen, presenting many challenges [1–8]. Theoretically, the bound-state perturbative theory is commonly used to estimate energy corrections beyond the Coulomb potential (see recent reviews and books [9–11] and the references therein). To reliably estimate these corrections, the effective Schrodinger-like equation [12] or the effective Dirac-like equations [13], which are derived exactly from the Bethe-Salpeter (BS) equation [14, 15] in quantum electrodynamics (QED) or non-relativistic quantum electrodynamics (NRQED) [16], should be employed, as there is no analytical solution for the physical BS equation.

Throughout history, various other methods have also been employed to investigate corrections beyond the Coulomb potential. These include the use of the Dirac equation with an effective potential [17], the external field approximation [9], the quasi-potential approach [18–20], and the Foldy-Wouthuysen transformation method [21–23], among others. However, in this work, we focus our discussion within the framework of the effective Schrodinger-like equation, which is derived exactly from the Bethe-Salpeter equation in QED [12].

In the bound-state perturbative theory, the interaction kernel is expanded order by order in terms of the coupling constant α_e , velocities $\vec{p}_i/m_{e,p}$, and m_e/m_p , where \vec{p}_i represents the three momenta of the system, and m_e and m_p denote the masses of the electron and proton, respectively. The expansion of the interaction kernel in terms of momenta implies that only contributions from low momenta are accurately considered, while contributions from high momenta need to be treated separately.

On the other hand, the wave functions in the Schrodinger equation with the Coulomb potential are valid for the entire momentum range. The integration of the wave functions and interaction kernels encompasses contributions from both low and high momenta. This can introduce additional ultraviolet (UV) divergences, which differ somewhat from the usual UV divergences in the scattering amplitudes arising from loop integrals in radiative corrections. To handle these UV divergences, regularization methods are employed [24–26]. These UV divergences eventually cancel each other out, and the final results are independent of the regularization procedure.

In this study, we use the one-photon-exchange (OPE) interaction as an example to perform a numerical calculation of the energy spectrum. Instead of expanding the OPE interaction in terms of momenta and m_e/m_p , we retain it in its full form. This approach

allows us to include all relativistic corrections at the order of α_e , and it avoids any additional UV divergences since the full OPE interaction kernel remains valid across the entire momentum range. This calculation can be regarded as a full result incorporating the OPE interaction, and it provides an interesting basis for comparison with the results obtained using the bound-state perturbative theory.

The paper is organized as follows: In Section II, we introduce the framework used in our calculations. In Section III, we present the numerical results for specific states, showcasing their properties. We also provide a brief discussion on the comparison of these numerical results with those obtained using the bound-state perturbative approach.

II. BASIC FORMULA

A. The effective Schrodinger-like equation

In QED, the bound states of the ep system in the center frame can be accurately described by the following effective Schrodinger-like equation [12]:

$$\left[P_0 - E_1^{(e)} - E_1^{(p)} \right] \phi_{\bar{\lambda}, \bar{\mu}}(\vec{p}_1) = \int \frac{d^3 \vec{p}_3}{(2\pi)^3} i \tilde{K}_{\bar{\lambda}\lambda, \bar{\mu}\mu}(\vec{p}_1, \vec{p}_3, P) \phi_{\lambda, \mu}(\vec{p}_3), \quad (1)$$

where $P = (P_0, \vec{0}) \equiv p_1 + p_2 = p_3 + p_4$, $p_{1,2,3,4}$ are the momenta of final and intermediate fermions as shown in Fig.1, $E_i^{(e)} \equiv \sqrt{\vec{p}_i^2 + m_e^2}$, $E_i^{(p)} \equiv \sqrt{\vec{p}_i^2 + m_p^2}$. The interaction kernel $\tilde{K}_{\bar{\lambda}\lambda, \bar{\mu}\mu}(\vec{p}_1, \vec{p}_3, P)$ is defined as

$$\tilde{K}_{\bar{\lambda}\lambda, \bar{\mu}\mu}(\vec{p}_1, \vec{p}_3, P) \equiv \frac{\bar{u}_{\bar{\alpha}}(\vec{p}_1, m_e, \bar{\lambda}) \bar{u}_{\bar{\beta}}(-\vec{p}_1, m_p, \bar{\mu})}{\sqrt{4E_1^{(e)} E_1^{(p)}}} \bar{K}_{\bar{\alpha}\alpha, \bar{\beta}\beta}(\vec{p}_1, \vec{p}_3, P) \frac{u_{\alpha}(\vec{p}_3, m_e, \lambda) u_{\beta}(-\vec{p}_3, m_p, \mu)}{\sqrt{4E_3^{(e)} E_3^{(p)}}}, \quad (2)$$

where

$$\bar{K}(\vec{p}_1, \vec{p}_3, P) \equiv \bar{K}(p_1, p_3, P) \Big|_{p_1^0 = p_3^0 = \tau_e P_0}, \quad (3)$$

$$\bar{K} \equiv [I - K_{\text{BS}}(G_0 - \bar{G}_0)]^{-1} K_{\text{BS}},$$

with $\tau_e \equiv m_e/(m_e + m_p)$ and K_{BS} the usual two-body BS irreducible kernel. Here, we directly make the assumption that the inverse $[I - K_{\text{BS}}(G_0 - \bar{G}_0)]^{-1}$ exists, and that \bar{K} can be expressed in a perturbative form as follows:

$$\bar{K}(p_1, p_3, P) = K_{\text{BS}}(p_1, p_3, P) + \int \frac{d^4 k}{(2\pi)^4} K_{\text{BS}}(p_1, k, P) [G_0(k, P) - \bar{G}_0(k, P)] K_{\text{BS}}(k, p_3, P) + \dots \quad (4)$$

where

$$\begin{aligned}
G_0(k, P) &\equiv S_{full}^{(e)}(k, m_e)S_{full}^{(p)}(P - k, m_p), \\
\bar{G}_0(k, P) &\equiv 2\pi i\delta(k^0) \left[\frac{\Lambda_+^{(e)}(\vec{k})\Lambda_+^{(p)}(-\vec{k})}{P_0 - E_e(\vec{k}) - E_p(\vec{k})} - \frac{\Lambda_-^{(e)}(\vec{k})\Lambda_-^{(p)}(-\vec{k})}{P_0 + E_e(\vec{k}) + E_p(\vec{k})} \right] \\
&\approx 2\pi i\delta(k^0) \frac{\Lambda_+^{(e)}(\vec{k})\Lambda_+^{(p)}(-\vec{k})}{P_0 - E_e(\vec{k}) - E_p(\vec{k})}.
\end{aligned} \tag{5}$$

In the above expressions, $S_{full}^{(e,p)}$ are the full propagators of the electron and proton [10], respectively, and $\Lambda_{\pm}^{(a)}(\vec{k})$ are

$$\Lambda_{\pm}^{(a)}(\vec{k}) \equiv \left[E^{(a)}(\vec{k})\gamma^0 \mp (\vec{k} \cdot \vec{\gamma} - m_a) \right]^{(a)} / 2E^{(a)}(\vec{k}), \tag{6}$$

with $E^{(a)}(\vec{k}) \equiv \sqrt{\vec{k}^2 + m_a^2}$.

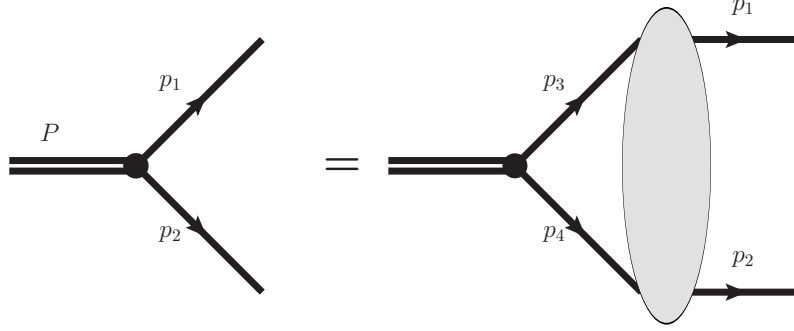


FIG. 1: Diagram for the BS equation.

In the leading order of α_e , $\vec{p}_i/m_{e,p}$, and m_e/m_p , the interaction kernel \tilde{K} can be chosen as

$$i\tilde{K}_{\lambda\lambda,\bar{\mu}\bar{\mu}}^{(0)}(\vec{p}_1, \vec{p}_3, P) \equiv \delta_{\lambda\lambda}\delta_{\bar{\mu}\bar{\mu}} \frac{-e^2}{|\vec{p}_1 - \vec{p}_3|^2} \frac{1}{[N(\vec{p}_1)N(\vec{p}_3)]^{1/2}}, \tag{7}$$

where

$$N(\vec{p}_i) \equiv \frac{[P_0 + E_i^{(e)} + E_i^{(p)}][P_0^2 - (E_i^{(e)} + E_i^{(p)})^2]}{2P_0 [P_0^2 - (m_e - m_p)^2]}. \tag{8}$$

By utilizing this effective interaction kernel and expanding the equation in terms of momenta and the bound energy, the effective Schrodinger-like equation Eq. (1) simplifies to the Schrodinger equation with the Coulomb potential. The contributions from interaction kernels involving higher orders of α_e , $\vec{p}_i/m_{e,p}$, and m_e/m_p beyond $\tilde{K}^{(0)}(\vec{p}_1, \vec{p}_3, P)$ can be estimated systematically using the bound-state perturbative theory, order by order. This approach can also be applied in NRQED, where the power counting and analytical calculations are more straightforward.

B. The full interaction kernel in the leading order of α_e

In the bound-state perturbative theory, the interaction kernels are expanded order by order in terms of $\vec{p}_i/m_{e,p}$, and the corresponding matrix elements often exhibit divergences. To handle these divergences, regular methods are employed during the intermediate calculations. It is important to note that these divergences arise naturally due to the slow decrease of the wave functions of the bound states with respect to momenta \vec{p}_i , whereas the expansion of the interaction kernels in terms of momenta is not valid in the high momentum region.

In this study, we adopt a different approach by not expanding the interaction kernel $\tilde{K}(\vec{p}_1, \vec{p}_3, P)$ in terms of $\vec{p}_i/m_{e,p}$ and m_e/m_p . Instead, we employ a numerical method to directly solve Eq. (1) using the leading-order α_e expression of $\tilde{K}(\vec{p}_1, \vec{p}_3, P)$.

In the leading order of α_e , only the OPE interaction contributes. As an approximation, we consider the proton to be a point-like particle in this study. Therefore, we have:

$$K_{\text{BS}, \bar{\alpha}\alpha, \bar{\beta}\beta}^{(\text{OPE})}(p_1, p_3, P) = (-ie\gamma_{\bar{\alpha}\alpha}^\mu)D_{\mu\nu}(p_1 - p_3)(+ie\gamma_{\bar{\beta}\beta}^\nu), \quad (9)$$

and

$$\bar{K}^{(\text{LO})}(\vec{p}_1, \vec{p}_3, P) = K_{\text{BS}}^{(\text{OPE})}(p_1, p_3, P) \Big|_{p_1^0 = p_3^0 = \tau_e P_0}. \quad (10)$$

Taking the Coulomb gauge, we have

$$\bar{K}_{\bar{\alpha}\alpha, \bar{\beta}\beta}^{(\text{LO})}(\vec{p}_1, \vec{p}_3, P) = (-ie\gamma_{\bar{\alpha}\alpha}^0) \frac{i}{|\vec{q}|^2} (+ie\gamma_{\bar{\beta}\beta}^0) + (-ie\gamma_{\bar{\alpha}\alpha}^i) \left[\frac{iq^i q^j}{|\vec{q}|^4} - \frac{i\delta^{ij}}{|\vec{q}|^2} \right] (+ie\gamma_{\bar{\beta}\beta}^j), \quad (11)$$

with $q = p_1 - p_3$. Here, $q^0 = 0$ due to the special choice of the momenta with $p_1^0 = p_3^0 = \tau_e P_0$.

After performing the necessary calculations, we obtain the following result:

$$\begin{aligned} i\tilde{K}_{\bar{\lambda}\lambda, \bar{\mu}\mu}(\vec{p}_1, \vec{p}_3, P) &\equiv \chi^{(e)\dagger}(\bar{\lambda})\chi^{(p)\dagger}(\bar{\mu})V(\vec{p}_1, \vec{p}_3)\chi^{(p)}(\mu)\chi^{(e)}(\lambda) \\ &= \sum_{i=1}^8 \frac{e^2 C_i [\chi^{(e)\dagger}(\bar{\lambda})\chi^{(p)\dagger}(\bar{\mu})T_i\chi^{(p)}(\mu)\chi^{(e)}(\lambda)]}{4z_1^2 \sqrt{E_1^{(e)} E_3^{(e)} E_1^{(p)} E_3^{(p)} X_1^{(e)} X_3^{(e)} X_1^{(p)} X_3^{(p)}}}, \end{aligned} \quad (12)$$

where χ is the Pauli spinor and

$$\begin{aligned}
T_1 &= 1, \\
T_2 &= i(\vec{p}_1 \times \vec{p}_3) \cdot \sigma^{(e)}, \\
T_3 &= i(\vec{p}_1 \times \vec{p}_3) \cdot \sigma^{(p)}, \\
T_4 &= \vec{p}_1 \cdot \sigma^{(e)} \vec{p}_1 \cdot \sigma^{(p)}, \\
T_5 &= \vec{p}_1 \cdot \sigma^{(e)} \vec{p}_3 \cdot \sigma^{(p)}, \\
T_6 &= \vec{p}_3 \cdot \sigma^{(e)} \vec{p}_1 \cdot \sigma^{(p)}, \\
T_7 &= \vec{p}_3 \cdot \sigma^{(e)} \vec{p}_3 \cdot \sigma^{(p)}, \\
T_8 &= \sigma^{(e)} \cdot \sigma^{(p)},
\end{aligned} \tag{13}$$

and

$$\begin{aligned}
C_1 &= (z_2 - z_1)(\vec{p}_1 \cdot \vec{p}_3)^2 - z_1 z_3 \vec{p}_1 \cdot \vec{p}_3 - z_2 |\vec{p}_1|^2 |\vec{p}_3|^2 - z_1 X_1^{(e)} X_3^{(e)} X_1^{(p)} X_3^{(p)}, \\
C_2 &= -(E_1^{(e)} + E_3^{(e)})(X_1^{(p)} + X_3^{(p)}) \vec{p}_1 \cdot \vec{p}_3 + z_1 \vec{p}_1 \cdot \vec{p}_3 + (m_e z_1 + t_e)(X_1^{(p)} + X_3^{(p)}) + z_1 X_1^{(p)} X_3^{(p)}, \\
C_3 &= -(E_1^{(p)} + E_3^{(p)})(X_1^{(e)} + X_3^{(e)}) \vec{p}_1 \cdot \vec{p}_3 + z_1 \vec{p}_1 \cdot \vec{p}_3 + (m_p z_1 + t_p)(X_1^{(e)} + X_3^{(e)}) + z_1 X_1^{(e)} X_3^{(e)}, \\
C_4 &= 2E_3^{(e)} E_3^{(p)} \vec{p}_1 \cdot \vec{p}_3 + E_1^{(e)}(E_1^{(p)} - E_3^{(p)}) |\vec{p}_3|^2 - E_3^{(e)}(m_p z_1 + t_p) - m_e X_3^{(p)} z_1, \\
C_5 &= -\vec{p}_1 \cdot \vec{p}_3 [E_1^{(e)}(E_1^{(p)} + E_3^{(p)}) + E_3^{(e)}(E_3^{(p)} - E_1^{(p)})] + E_1^{(e)} E_3^{(p)} z_4 + E_1^{(e)} m_p z_1 + m_e X_3^{(p)} z_1, \\
C_6 &= -\vec{p}_1 \cdot \vec{p}_3 [E_1^{(e)}(E_1^{(p)} - E_3^{(p)}) + E_3^{(e)}(E_3^{(p)} + E_1^{(p)})] + E_3^{(e)} E_1^{(p)} z_4 + E_3^{(e)} m_p z_1 + m_e X_1^{(p)} z_1, \\
C_7 &= 2E_1^{(e)} E_1^{(p)} \vec{p}_1 \cdot \vec{p}_3 + E_3^{(e)}(E_3^{(p)} - E_1^{(p)}) |\vec{p}_1|^2 - E_1^{(e)}(m_p z_1 + t_p) - m_e X_1^{(p)} z_1, \\
C_8 &= (-\vec{p}_1 \cdot \vec{p}_3 (E_1^{(e)} + E_3^{(e)}) + m_e z_1 + t_e)(-\vec{p}_1 \cdot \vec{p}_3 (E_1^{(p)} + E_3^{(p)}) + m_p z_1 + t_p),
\end{aligned} \tag{14}$$

with

$$\begin{aligned}
X_i^{(a)} &\equiv E_i^{(a)} + m_a, \\
z_1 &\equiv |\vec{p}_1|^2 + |\vec{p}_3|^2 - 2\vec{p}_1 \cdot \vec{p}_3, \\
z_2 &\equiv (X_1^{(e)} + X_3^{(e)})(X_1^{(p)} + X_3^{(p)}), \\
z_3 &\equiv X_1^{(e)} X_3^{(e)} + X_1^{(p)} X_3^{(p)}, \\
z_4 &\equiv |\vec{p}_1|^2 + |\vec{p}_3|^2, \\
t_e &\equiv E_1^{(e)} |\vec{p}_3|^2 + E_3^{(e)} |\vec{p}_1|^2, \\
t_p &\equiv E_1^{(p)} |\vec{p}_3|^2 + E_3^{(p)} |\vec{p}_1|^2.
\end{aligned} \tag{15}$$

By expanding the potential V in terms of $\vec{p}_i/m_{e,p}$, it can be verified that the leading-order term corresponds to the Coulomb potential, while the next-leading-order terms

correspond to the Breit potential. The higher-order terms correspond to the effective potential beyond the Breit potential. Similarly, the expansion results also correspond to the amplitude in NRQED at the leading order of α_e , with higher orders of $\vec{p}_i/m_{e,p}$.

C. Energy correction in the bound-state perturbative theory

Expanding $H_p \equiv V + (E_1^{(e)} + E_1^{(p)} - m_e - m_p)(2\pi)^3\delta^3(\vec{p}_1 - \vec{p}_3)$ in terms of momenta yields the following results:

$$H_p = H_p^{(2)} + H_p^{(4)} + \dots, \quad (16)$$

where

$$\begin{aligned} H_p^{(2)} &= \left[\frac{\vec{p}_1^2}{2m_e} + \frac{\vec{p}_1^2}{2m_p} \right] (2\pi)^3 \delta^3(\vec{p}_1 - \vec{p}_3) - \frac{e^2}{\vec{q}^2}, \\ H_p^{(4)} &= H_{p,0}^{(4)} + H_{p,1}^{(4)} + H_{p,2}^{(4)}, \end{aligned} \quad (17)$$

with

$$\begin{aligned} H_{p,0}^{(4)}(\vec{p}_1, \vec{q}) &= - \left[\frac{\vec{p}_1^4}{8m_e^3} + \frac{\vec{p}_1^4}{8m_p^3} \right] (2\pi)^3 \delta^3(\vec{p}_1 - \vec{p}_3) + \frac{e^2}{8} \left[\frac{1}{m_e^2} + \frac{1}{m_p^2} \right] + \frac{e^2}{m_e m_p} \left[\frac{(\vec{q} \cdot \vec{p}_1)^2}{\vec{q}^4} - \frac{\vec{p}_1^2}{\vec{q}^2} \right], \\ H_{p,1}^{(4)}(\vec{p}_1, \vec{q}) &= \left[\frac{e^2}{4m_e^2} + \frac{e^2}{2m_e m_p} \right] \frac{1}{\vec{q}^2} i\sigma^{(e)} \cdot (\vec{q} \times \vec{p}_1), \\ H_{p,2}^{(4)}(\vec{p}_1, \vec{q}) &= - \frac{e^2}{4m_e m_p} \left[\frac{\sigma^{(e)} \cdot \vec{q} \sigma^{(p)} \cdot \vec{q}}{\vec{q}^2} - \sigma^{(e)} \cdot \sigma^{(p)} \right] + \left[\frac{e^2}{4m_p^2} + \frac{e^2}{2m_e m_p} \right] \frac{i\sigma^{(p)} \cdot (\vec{q} \times \vec{p}_1)}{\vec{q}^2}. \end{aligned} \quad (18)$$

Here, $H_p^{(4)}$ corresponds to the Breit potential in momentum space.

In the perturbative bound-state theory, the energy contribution of the hydrogen due to the OPE interaction can be written as:

$$E_n = E_n^{(2)} + E_n^{(4)} + E_n^{(6)} + \dots \quad (19)$$

where

$$\begin{aligned} E_n^{(2)} &= \langle n, l, j, F | H^{(2)} | n, l, j, F \rangle = -\frac{\alpha_e^2 \mu}{2n^2}, \\ E_n^{(4)} &= \langle n, l, j, F | H^{(4)} | n, l, j, F \rangle, \\ E_n^{(6)} &= \langle n, l, j, F | H^{(4)} Q (E_n^{(2)} - H^{(2)})^{-1} Q H^{(4)} | n, l, j, F \rangle + \langle n, l, j, F | H^{(6)} | n, l, j, F \rangle. \end{aligned} \quad (20)$$

Here, $\alpha_e \equiv \frac{e^2}{4\pi}$, $\mu = \frac{m_e m_p}{m_e + m_p}$ and Q is a projection operator on a subspace orthogonal to $|n, l, j, F\rangle$.

The calculation of $E_{n,i}^{(4)}$ can be performed directly, and the analytic results are expressed as:

$$E_n^{(4)} = E_{n,0}^{(4)} + E_{n,1}^{(4)} + E_{n,2}^{(4)}, \quad (21)$$

where

$$\begin{aligned} E_{n,0}^{(4)} &= \frac{\alpha_e^4 \mu}{2n^3} \left[1 - \frac{(2-6n)\mu}{n(m_e + m_p)} \right], \\ E_{n,1}^{(4)} &= \frac{2\alpha_e^4 \mu m_p (2m_e + m_p)}{n^3 (m_e + m_p)^2} \frac{j-l}{(2l+1)(2j+1)} (1 - \delta_{0l}), \\ E_{n,2}^{(4)} &= \frac{\alpha_e^4 \mu^2}{n^3 (m_e + m_p)} \frac{1}{(2l+1)(2F+1)} \begin{cases} \frac{4}{3} [F^2 + F - \frac{3}{2}] \delta_{0l}, & l = 0 \\ -\frac{1}{l}, & l \neq 0, F = l + 1 \\ -\frac{1}{(l+1)}, & l \neq 0, F = l - 1. \end{cases} \end{aligned} \quad (22)$$

The calculation of $E_n^{(6)}$ is somewhat complex [27–30], and there is a UV divergence in the middle matrix elements for the S wave, as explained above. In this work, we will not compare these results.

D. The form of the wave function

The wave function in Eq. (1) can be written as:

$$\phi_{\bar{\lambda}, \bar{\mu}}(\vec{p}_1) = \sum_{\bar{\alpha}, \bar{\beta}} \chi_{\bar{\alpha}}^{(e)\dagger}(\bar{\lambda}) \chi_{\bar{\beta}}^{(p)\dagger}(\bar{\mu}) \Phi_{\bar{\alpha}, \bar{\beta}}(\vec{p}_1), \quad (23)$$

which results in the following equation:

$$\left[P_0 - E_1^{(e)} - E_1^{(p)} \right] \Phi_{\bar{\alpha}, \bar{\beta}}(\vec{p}_1) = \int \frac{d^3 \vec{p}_3}{(2\pi)^3} V_{\bar{\alpha}\alpha, \bar{\beta}\beta}(\vec{p}_1, \vec{p}_3) \Phi_{\alpha, \beta}(\vec{p}_3). \quad (24)$$

To compare with the results in the references, we label the state of the system as nL_j^F . For $F = j \pm \frac{1}{2} = l \pm 1$, we have the following form for $\Phi_{\alpha, \beta}(\vec{p}_3)$:

$$\Phi_{\alpha, \beta}(\vec{p}_3) = \sum_{s_z^e, s_z^p} \chi_{\alpha}(s_z^p) \chi_{\beta}(s_z^e) \langle jj_z | lm, s s_z^e \rangle \langle FF_z | jj_z, s s_z^p \rangle \Phi_{nlm}(\vec{p}_3). \quad (25)$$

When the effective potential V does not include spin-dependent terms, the above form of the wave function gives the same result as the following form:

$$\Phi_{\alpha, \beta}(\vec{p}_3) \rightarrow \Phi_{nlm}(\vec{p}_3). \quad (26)$$

We would also like to mention that the above form of the wave functions corresponds to the quantum numbers in non-relativistic quantum mechanics. When discussing states in QED, one can consider J^P as good quantum numbers to determine the most general form of the wave function $\Phi_{\alpha,\beta}$ for solving the equation. In this case, effects such as the mixing of S wave and D wave naturally appear. However, in this work, we limit our discussion to the relativistic effects when considering the above form of the wave functions.

E. Numerical method

To calculate the energy contributions beyond the bound-state perturbative theory, we expand $\Phi_{nlm}(\vec{p})$ as:

$$\Phi_{nlm}(\vec{p}) \approx \sum_{i=l+1}^{n_{max}} c_{ni} \phi_{ilm}^{(0)}(\vec{p}) \equiv \sum_{i=l+1}^{n_{max}} c_{ni} \phi_{il}^{(0)}(|\vec{p}|) Y_{lm}(\Omega_{\vec{p}}), \quad (27)$$

where

$$\phi_{il}^{(0)}(|\vec{p}|) \equiv \bar{p}^l a^{3/2} N_{il} \frac{l!}{\sqrt{2\pi}} \times \frac{4^{l+1}}{(\bar{p}^2 + \delta^2)^{l+2}} C_{n-l-1}^{l+1} \left(\frac{\bar{p}^2 - \delta^2}{\bar{p}^2 + \delta^2} \right), \quad (28)$$

and

$$N_{il} = \frac{2}{i^2} \sqrt{\frac{(i-l-1)!}{(i+l)!}}, \quad \bar{p} = ap, \quad (29)$$

with $a = \frac{1}{\mu e^2}$ the Bohr radius.

By choosing a specific value of n_{max} , one can calculate the following matrix:

$$\int d^3\vec{p}_1 \Phi_{\bar{\alpha},\bar{\beta};i}^{(0)\dagger}(\vec{p}_1) [E_1^{(e)} + E_1^{(p)}] \delta_{\bar{\alpha}\alpha} \delta_{\bar{\beta}\beta} \Phi_{\alpha,\beta;i}^{(0)}(\vec{p}_1) + \int \frac{d^3\vec{p}_1 d^3\vec{p}_3}{(2\pi)^3} \Phi_{\bar{\alpha},\bar{\beta};i}^{(0)\dagger}(\vec{p}_1) V_{\bar{\alpha}\alpha,\bar{\beta}\beta}(\vec{p}_1, \vec{p}_3) \Phi_{\alpha,\beta;i}^{(0)}(\vec{p}_3), \quad (30)$$

where $\Phi_{\alpha,\beta;i}^{(0)}(\vec{p}_1)$ is simply $\Phi_{\alpha,\beta}(\vec{p}_1)$ in Eq. (25) after replacing $\Phi_{nlm}(\vec{p}_1)$ with $\phi_{il}^{(0)}(|\vec{p}_1|) Y_{lm}$. The integration over the angles $\Omega_{\vec{p}_1}$ and $\Omega_{\vec{p}_3}$ can be performed analytically, while the integration over $|\vec{p}_1|$ and $|\vec{p}_3|$ can be done numerically with high precision. After diagonalizing this matrix, the energy spectrum $E_n \equiv P0, n - m_e - m_p$ is obtained approximately.

III. NUMERICAL RESULTS AND DISCUSSION

In our numerical calculation, we set $n_{max} = 100$, and the physical constants are taken as $m_e = 0.510998950$ MeV, $m_p = 938.27208816$ MeV, and $\alpha_e = \frac{1}{137.035999084}$. The relative precision of the numerical calculation for each matrix element reaches 10^{-20} , ensuring that

the absolute precision of the matrix elements is better than 10^{-18} eV. This guarantees the reliability of the numerical results. The numerical precision is also tested for the matrix elements involving the Coulomb and Breit potentials.

To compare the results with those obtained using bound-state perturbative theory, we decompose the effective potential into three terms as follows:

$$V \equiv V_0 + V_1 + V_2, \quad (31)$$

where V_0 is spin-independent, V_1 depends only on the electron spin, and V_2 depends on the proton spin. We label the corresponding energy contributions due to $V_0, V_0 + V_1, V_0 + V_1 + V_2$ as $E_{n,0}, E_{n,1}, E_{n,2}$, respectively. The contributions beyond the Breit potential are expressed by the following quantities:

$$\begin{aligned} \Delta E_{n,0} &\equiv E_{n,0} - E_n^{(2)} - E_{n,0}^{(4)}, \\ \Delta E_{n,1} &\equiv E_{n,1} - E_n^{(2)} - E_{n,0}^{(4)} - E_{n,1}^{(4)}, \\ \Delta E_{n,2} &\equiv E_{n,2} - E_n^{(2)} - E_{n,0}^{(4)} - E_{n,1}^{(4)} - E_{n,2}^{(4)}. \end{aligned} \quad (32)$$

n \backslash peV	$\Delta E_{n,0}(S)$	$\Delta E_{n,0}(P)$	$\Delta E_{n,0}(D)$
$n = 1$	-2349361	-	-
$n = 2$	-289552	813	-
$n = 3$	-85154	424	13
$n = 4$	-35738	242	16
$n = 5$	-18225	151	14

TABLE I: The numeric results for the energy corrections $\Delta E_{n,0}(l)$, where the unit is peV (10^{-12} eV).

We present the numeric results for $\Delta E_{n,i}$ in Tabs. I, II and III, respectively, where $l = 0, 1, 2$ or S, P, D waves, $j = l + 1/2$ and $F = l + 1$ are considered. For the purpose of a more direct comparison, we also provide the contributions with specific orders as follows:

$$\begin{aligned} \alpha_e^5 \mu &\sim 11 \mu\text{eV}, \\ \alpha_e^6 \mu &\sim 77 \text{neV}, \\ \alpha_e^6 \mu \frac{m_e}{m_p} &\sim 42 \text{peV}. \end{aligned} \quad (33)$$

n \ peV	$\Delta E_{n,1}(S)$	$\Delta E_{n,1}(P)$	$\Delta E_{n,1}(D)$
$n = 1$	-2349361	-	-
$n = 2$	-289552	-44	-
$n = 3$	-85154	50	3
$n = 4$	-35738	48	6
$n = 5$	-18225	37	6

TABLE II: The numeric results for the energy correction $\Delta E_{n,1}(l)$ with $j = l + 1/2$, where the unit is peV (10^{-12}eV).

n \ peV	$\Delta E_{n,2}(S)$	$\Delta E_{n,2}(P)$	$\Delta E_{n,2}(D)$
$n = 1$	-2357360	-	-
$n = 2$	-290555	-45	-
$n = 3$	-85452	50	3
$n = 4$	-35864	48	6
$n = 5$	-18289	37	6

TABLE III: The numeric results for the energy correction $\Delta E_{n,2}(l)$ with $F = j+1/2 = l+1$, where the unit is peV (10^{-12}eV).

The results in Tab. I, II and III clearly demonstrate a notable property whereby the contributions in the S wave are significantly larger than those in the P and D waves.

In terms of magnitude, the contributions $\Delta E_{n,0}(S)$ are approximately $-\frac{\alpha_e^5 \mu}{4.5n^3} \sim -\frac{30\alpha_e^6 \mu}{n^3}$, which are larger than the contributions at the order of $\frac{\alpha_e^6 \mu}{n^3}$. The contributions $\Delta E_{n,0}(P)$ are on the order of $\frac{\alpha_e^6 \mu}{20n^2}$. On the other hand, the contributions $\Delta E_{n,0}(D)$ weakly depend on n and are much smaller than $\alpha_e^6 \mu$.

The results for $\Delta E_{n,1}(S)$ and $\Delta E_{n,2}(S)$ are similar to $\Delta E_{n,0}(S)$, indicating that the contributions from spin-independent terms are most significant for the S wave. This is expected, as the contributions from electron spin are zero for the S wave, and the contributions from proton spin are greatly suppressed.

The results for $\Delta E_{n,1}(P)$ and $\Delta E_{n,2}(P)$ are similar to each other and significantly differ from $\Delta E_{n,0}(P)$. This indicates that in the P wave, the contributions from the electron

spin are of the same order as the spin-independent contributions. The spin-dependent contributions in the D wave are similar to those in the P wave.

To illustrate the contributions more explicitly, we define the following terms:

$$\begin{aligned}\Delta E_n^{fin} &\equiv \Delta E_{n,1} - \Delta E_{n,0} = E_{n,1} - E_{n,0} - E_{n,1}^{(4)}, \\ \Delta E_n^{hyf} &\equiv \Delta E_{n,2} - \Delta E_{n,1} = E_{n,2} - E_{n,1} - E_{n,2}^{(4)}.\end{aligned}\tag{34}$$

These terms reflect the corrections to the fine structure and hyperfine structure beyond the Breit potential, respectively.

n \backslash peV	$\Delta E_n^{fin}(S)$	$\Delta E_n^{fin}(P)$	$\Delta E_n^{fin}(D)$
$n = 1$	0	-	-
$n = 2$	0	-857	-
$n = 3$	0	-374	-10
$n = 4$	0	-194	-10
$n = 5$	0	-114	-8

TABLE IV: Numeric results for the energy correction $\Delta E_n^{fin}(l)$ with $j = l + 1/2$, where the unit is peV (10^{-12} eV).

n \backslash peV	$\Delta E_n^{hyf}(S)$	$\Delta E_n^{hyf}(P)$	$\Delta E_n^{hyf}(D)$
$n = 1$	-7999	-	-
$n = 2$	-1003	-0.66	-
$n = 3$	-298	-0.27	-0.007
$n = 4$	-126	-0.14	-0.007
$n = 5$	-65	-0.08	-0.005

TABLE V: Numeric results for the energy correction $\Delta E_n^{hyf}(l)$ with $F = l + 1$, where the unit is peV (10^{-12} eV).

The numeric results for ΔE_n^{fin} and ΔE_n^{hyf} are presented in Tab. IV and V, respectively. The numerical results in Tab. IV indicate that the contributions to the fine structure beyond the Breit potential are approximately $-\frac{\alpha_e^6 \mu}{22n^2}$ in the P wave and around -10 peV

in the D wave. These values are much smaller compared to the contributions of $-\frac{\alpha_e^6 \mu}{n^2}$. The numeric results in Tab. V show that the contributions to the hyperfine structure beyond the Breit potential are approximately $-\frac{200\alpha_e^6 \mu}{n^3} \frac{m_e}{m_p}$ for the S wave, while the contributions are negligible for the P wave and D wave cases.

To demonstrate the uncertainty arising from the approximation of finite n_{\max} , we plot $\Delta E_{l+1,0}(l, n_{\max})$ as a function of n_{\max} in Fig. 2. The results clearly indicate that the uncertainty is smaller than 0.5peV when $n_{\max} > 60$, suggesting that the approximation is reliable.

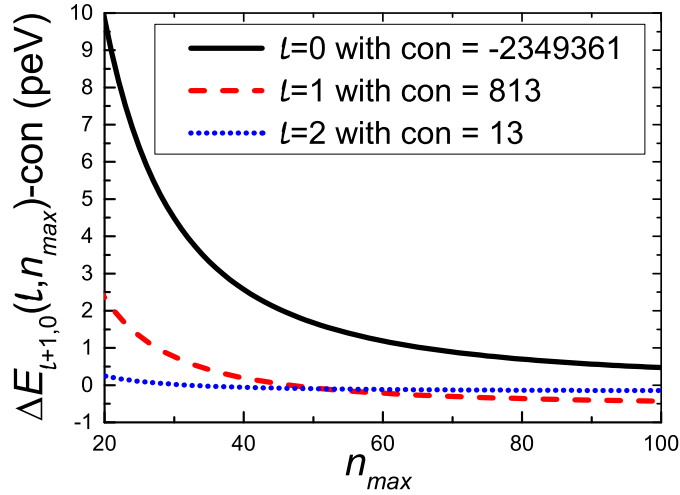


FIG. 2: Numeric results for $\Delta E_{l+1,0}(l, n_{\max})$ vs. n_{\max} with $l = 0, 1$ and 2 , where the unit is peV (10^{-12}eV).

In our calculation, we do not expand the OPE interaction kernel order by order in momenta, but instead solve the effective Schrodinger-like equation using numerical method. This approach enables us to include all contributions from ladder diagrams with the approximated propagator \bar{G}_0 and the full photon propagator, while excluding the crossed diagrams. Consequently, the comparison of our results with those obtained from bound-state perturbation theory is not straightforward.

For a consistent comparison between the two approaches, one would need to separate the contributions in bound-state perturbation theory based on the diagram types and momentum regions, and then compare them with our results to assess the relativistic contributions obtained through the expansion in bound-state perturbation theory. How-

ever, such a direct separation and comparison fall beyond the scope of this work.

In summary, the effective potential associated with the full OPE interaction in momentum space is expressed through eight scalar functions. The expansions of these scalar functions directly correspond to the $ep \rightarrow ep$ amplitude in NRQED or the quasi-potential at order α_e and any desired order of momenta. Our precise numerical calculations suggest that it is possible to capture all relativistic contributions using this method. Extending these calculations to positronium, muonic hydrogen, and cases involving nuclear structure and radiative corrections would be interesting directions for future research.

IV. ACKNOWLEDGMENTS

H.Q.Z. would like to thank Zhi-Hui Guo for his helpful suggestions and discussions. This work is funded in part by the National Natural Science Foundations of China under Grants No. 12075058, No. 12150013.

-
- [1] Pohl R, *et al.*, Nature **466**, 213 (2010).
 - [2] Aldo Antognini, *et al.*, Science **339**, 417 (2013).
 - [3] A. Beyer, L. Maisenbacher, A. Matveev, R. Pohl, K. Khabarova, A. Grinin, T. Lamour, D.C. Yost, T.W. Hansch, N. Kolachevsky et al., Science 358, 79 (2017).
 - [4] H. Fleurbaey, S. Galtier, S. Thomas, M. Bonnaud, L. Julien, F. m. c. Biraben, F. m. c. Nez, M. Abgrall, J. Guena, Phys. Rev. Lett. 120, 183001 (2018).
 - [5] N. Bezginov, T. Valdez, M. Horbatsch, A. Marsman, A.C. Vutha, E.A. Hessels, Science 365, 1007 (2019).
 - [6] A. Grinin, A. Matveev, D.C. Yost, L. Maisenbacher, V. Wirthl, R. Pohl, T.W. Hansch, T. Udem, Science 370, 1061 (2020).
 - [7] A. D. Brandt, S. F. Cooper, C. Rasor, Z. Burkley, D. C. Yost and A. Matveev, Phys. Rev. Lett. **128**, 023001 (2022).
 - [8] R. G. Bullis, C. Rasor, W. L. Tavis, S. A. Johnson, M. R. Weiss and D. C. Yost, Phys. Rev. Lett. **130**, 203001 (2023).

- [9] M. I. Eides, H. Grotch and V. A. Shelyuto, “Theory of Light Hydrogenic Bound States,” Springer Tracts Mod. Phys. **222**,1 (2007), ISBN 978-3-540-45269-0, 978-3-540-45270-6.
- [10] U. D. Jentschura and G. S. Adkins, “Quantum Electrodynamics: Atoms, Lasers and Gravity,” World Scientific, 2022, ISBN 978-981-12-5225-9, 978-981-12-5227-3.
- [11] K. Pachucki, V. Lensky, F. Hagelstein, S. S. Li Muli, S. Bacca and R. Pohl, Rev. Mod. Phys. **96**, 015001 (2024).
- [12] H. W. E. Caswell and G. P. Lepage, Phys. Rev. A **18**, 810 (1978).
- [13] G. P. Lepage, Phys. Rev. A **16**, 863 (1977).
- [14] E. E. Salpeter and H. A. Bethe, Phys. Rev. **84**, 1232 (1951).
- [15] M. Gell-Mann and F. Low, Phys. Rev. **84**, 350 (1951).
- [16] W. Caswell and G. Lepage, Phys. Lett. B **167**, 437 (1986).
- [17] H. Grotch and D. r. Yennie, Rev. Mod. Phys. **41**, 350 (1969).
- [18] R. N. Faustov, A. P. Martynenko, Teor.Mat.Fiz. **64**,179 (1985).
- [19] R. N. Faustov, A. P. Martynenko, Zh.Eksp.Teor.Fiz. **115**, 1221 (1999).
- [20] A. P. Martynenko, Jour. Exp. Theor. Phys. **101**, 1021 (2005).
- [21] L. L. Foldy and S. A. Wouthuysen, Phys. Rev. **78**, 29 (1950).
- [22] K. Pachucki, Phys. Rev. A **71**, 012503 (2005).
- [23] W. Zhou, X. Mei and H. Qiao, J. Phys. B **56**, 045001 (2023).
- [24] K. Pachucki, Phys. Rev. A **56**, 297 (1997).
- [25] A. Czarnecki, K. Melnikov and A. Yelkhovsky, Phys. Rev. A **59**, 4316 (1999).
- [26] G. S. Adkins, M. F. Alam, C. Larison and R. Sun, Phys. Rev. A **101**, 042511 (2020).
- [27] Z. X. Zhong, W. P. Zhou and X. S. Mei, Phys. Rev. A **98**, no.3, 032502 (2018) [erratum: Phys. Rev. A **101**, no.6, 069901 (2020)].
- [28] W. Zhou, X. Mei and H. Qiao, Phys. Rev. A **100**, 012513 (2019).
- [29] M. Haidar, Z. X. Zhong, V. I. Korobov and J. P. Karr, Phys. Rev. A **101**, 022501 (2020).
- [30] G. S. Adkins, J. Gomprecht, Y. Li and E. Shinn, Phys. Rev. Lett. **130**, 023004 (2023).